JOURNAL OF GEOPHYSICAL RESEARCH, VOL. 113, C04039, doi:10.1029/2007JC004346, 2008

Formation and export of dense shelf water from the Adélie Depression, East Antarctica

G. D. Williams,[1] N. L. Bindoff,[1,2] S. J. Marsland,[3,4] and S. R. Rintoul[4,5]

Received 21 May 2007; revised 7 September 2007; accepted 28 November 2007; published 29 April 2008.

[1] Coastal polynyas in the Adélie Depression are an important source of Antarctic Bottom Water to the Australian-Antarctic Basin. We present time series (April 1998 to May 1999 and August 1999 to February 2000) of data from temperature-salinity sensors, in both the Adélie Depression and the known outflow region of the Adélie Sill, to describe the annual cycle of shelf water densities. From April through September, salinification beneath the polynya produces dense shelf waters. During September–October, shelf water densities in the depression peak at 27.94 kg m^{-3}, and the cooling and freshening signature of Ice Shelf Water is observed north of Buchanan Bay. In November–December, shelf water densities decrease as intrusions of warm and relatively fresh modified Circumpolar Deep Water enter east of the Adélie Sill. From January–March the surface layer is conditioned by the cooling of the atmosphere, which overturns the upper water column. At the Adélie Sill, observed daily mean currents were approximately 10 cm s^{-1} with intense instantaneous currents greater than 50 cm s^{-1} at the sill depth. Using an idealized outflow region with a rectangular cross-sectional area (6×10^6 m^2), we present the first estimates of shelf water export by potential density class. Assuming shelf water with a minimum density of 27.88 kg m^{-3} has sufficient negative buoyancy for downslope mixing and a fourfold volume increase (1:3 mixing ratio) from entrainment, the dense shelf water export of 0.1–0.5 Sv results in an annual average production of bottom water in this region of between 0.4 and 2.0 Sv. The wide range in bottom water estimate results from data limitations, and a narrowing of this range requires further mooring observations.

Citation: Williams, G. D., N. L. Bindoff, S. J. Marsland, and S. R. Rintoul (2008), Formation and export of dense shelf water from the Adélie Depression, East Antarctica, *J. Geophys. Res.*, *113*, C04039, doi:10.1029/2007JC004346.

1. Introduction

[2] Antarctic Bottom Water (AABW) is the cold, dense water mass that occupies the base of the Southern Hemisphere oceans. Dense water forms through atmospheric cooling, brine rejection from sea ice growth, and ocean/ice shelf interactions in discrete locations around the Antarctic continent. With suitable bathymetry and sufficient buoyancy loss, dense Antarctic shelf waters can mix down the continental slope into the abyssal layers of the adjacent ocean basins forming AABW. The volume transport associated with the production and circulation of AABW influences the global meridional redistribution of heat and it is an important component of the global climate [*Orsi et al.*, 2002; *Jacobs*, 2004]. There are at least three major sources of AABW: the Weddell Sea, the Ross Sea, and Adélie Land Coast. The distinct pathways from each source define the water mass properties of the global ocean's deep basins to the north.

[3] The Australian-Antarctic Basin (80°–150°E) is supplied by two sources of AABW (Figure 1a). The relatively warmer and more saline Ross Sea Bottom Water (RSBW) from the east mixes with the colder, fresher and oxygen-rich Adélie Land Bottom Water (ALBW) that is formed locally in this region [*Whitworth*, 2002; *Rintoul*, 1998; *Fukamachi et al.*, 2000; *Whitworth*, 2002; *Aoki et al.*, 2005]. A freshening trend has been reported in the abyssal layer of the Australian-Antarctic Basin over the 1950–2000 period of observations [*Whitworth*, 2002; *Jacobs et al.*, 2002; *Jacobs*, 2004, 2006; *Aoki et al.*, 2005; *Rintoul*, 2007]. The cooling signal has been interpreted as an increasing influence of the ALBW source, but the freshening signal is more complicated to interpret because of the relatively warm and more saline RSBW entering the basin from the east has also been reported to have freshened significantly in the last 50 years [*Jacobs*, 2004].

[4] ALBW forms from the export of dense shelf waters produced beneath coastal polynyas [*Gordon and Tchernia*,

[1]Antarctic Climate and Ecosystems Cooperative Research Centre, Hobart, Tasmania, Australia.
[2]Also at CSIRO Marine and Atmospheric Research, Hobart, Tasmania, Australia.
[3]CSIRO Marine and Atmospheric Research, Aspendale, Victoria, Australia.
[4]Also at Antarctic Climate and Ecosystems Cooperative Research Centre, Hobart, Tasmania, Australia.
[5]CSIRO Marine and Atmospheric Research, Hobart, Tasmania, Australia.

0148-0227/08/2007JC004346$09.00

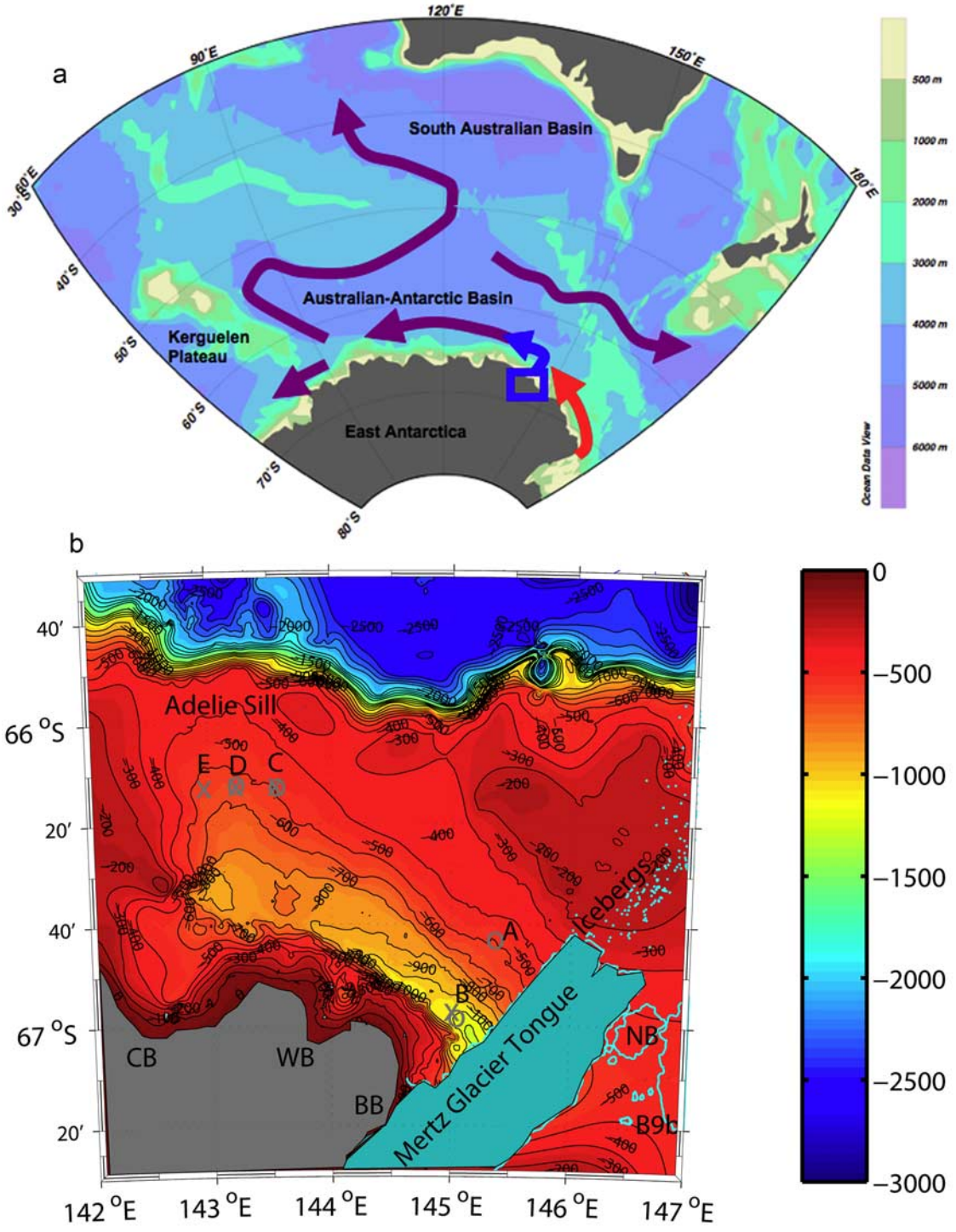

Figure 1. (a) Large-scale map of the East Antarctic sector of the Southern Ocean from General Bathymetric Chart of the Oceans with major Antarctic Bottom Water pathways (Ross Sea Bottom Water (red), Adélie Land Bottom Water (blue), and Ross Sea Bottom Water (RSBW)/Adélie Land Bottom Water (ALBW) mixture (purple) after *Rintoul* [2007]). (b) Survey-scale map of the Adélie Depression. Bathymetry data are from the 0.01° data set of *Porter-Smith* [2003]. Mooring locations are labeled from A through E and marked in grey with crosses for the 1998–1999 array and circles for the 1999–2000 array. Also shown is the Adélie Sill, Commonwealth Bay (CB), Watt Bay (WB), Buchanan Bay (BB), the Mertz Glacier Tongue, grounded icebergs, a remnant Ninnis Glacier iceberg (NB) and iceberg B9b. Ice features are as digitized from a RadarSat image taken in October 1999.

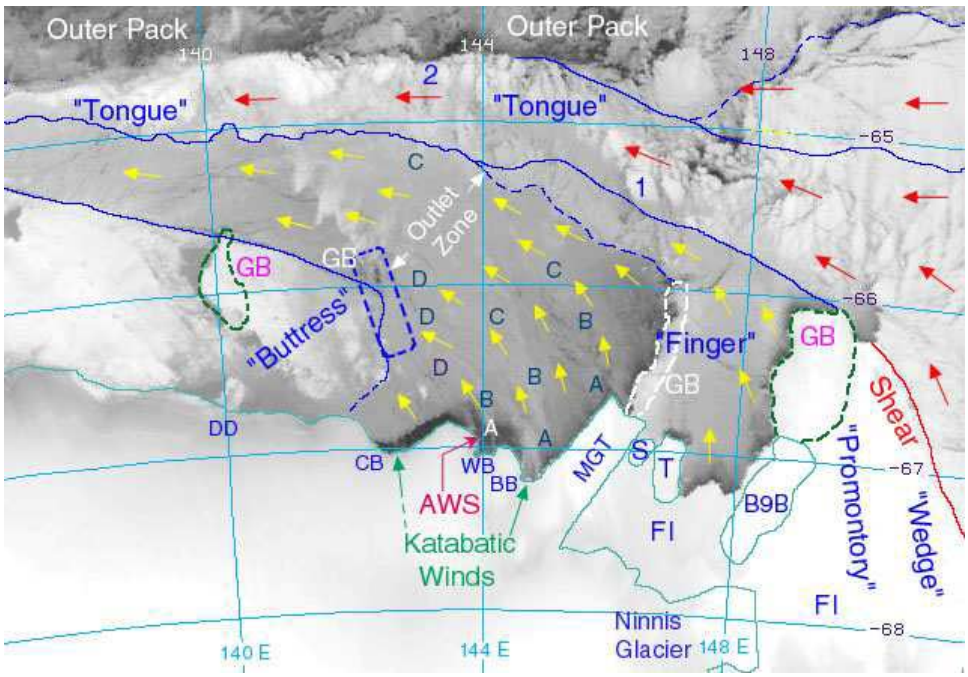

Figure 2. Mertz polynya region from an advanced very high resolution radiometer image taken on 14 July 1999. Abbreviations are as follows: GB, grounded bergs; FI, fast ice; B9B, iceberg B9B; S and T, grounded bergs; BB, Buchanan Bay; WB, Watt Bay; CB, Commonwealth Bay; and DD, Dumont Dúrville. Vectors are derived from buoy and satellite tracked floes, with yellow and red denoting new and old sea ice, respectively. For further details see *Massom et al.* [2001].

1972; *Rodman and Gordon*, 1982; *Rintoul*, 1998; *Fukamachi et al.*, 2000; *Bindoff et al.*, 2000a, 2001; *Williams and Bindoff*, 2003; *Morales Maqueda et al.*, 2004], in particular the Mertz Glacier polynya system located over the Adélie Depression (142–147°E, Figure 1b). Direct observations of the formation and export of dense shelf water from the Adélie Depression or other source regions of AABW around Antarctica are rare. The first wintertime experiment in the Adélie Depression by ship in July–August 1999 confirmed this location as a region of intense sea ice growth (5–10 cm d^{-1}) and dense shelf water production [*Bindoff et al.*, 2001; *Williams and Bindoff*, 2003].

[5] *Massom et al.* [2001] detail the sea-ice regime of Adélie Land Coast (see Figure 2). There are two distinct regions of polynya formation: the "coastal" polynyas along the continent and the "flaw" polynya in the lee of the western edge of the Mertz Glacier [*Wendler et al.*, 1997; *Morales Maqueda et al.*, 2004]. The former is influenced more by the local katabatic winds, the latter by synoptic atmospheric forcing [*Massom et al.*, 2001].

[6] Observations show warm and relatively fresh modified Circumpolar Deep Water (MCDW) flowing southward across the shelf break into the Adélie Depression at 144°E and cold, high-salinity shelf water flowing out of the Adélie Sill at 143°E. A broad clockwise flow results, with inflow southeast into the depression and along the Mertz Glacier, and a return flow west along the coast and out through the Adélie Sill. An ocean/sea ice process modeling study by *Marsland et al.* [2004] showed a similar circulation. The overall circulation pattern for the Adélie Depression is summarized in Figure 3. *Williams and Bindoff* [2003] concluded the coastal bay polynya region to the west of the Mertz Glacier Tongue (MGT), as first described by *Wendler et al.* [1997], must be the source of the densest High-Salinity Shelf Water (HSSW) based on the most extreme HSSW being observed in the Adélie sill region. The contact of the densest HSSW with the base of the MGT produces Ice Shelf Water that ascends and provides a cold, freshwater signal in the upper shelf waters. Shelf waters at intermediate depths ($\leq$500 m) flow out of the Adélie Depression through the Adélie Sill.

[7] Using a high-resolution coupled sea ice and ocean model, *Marsland et al.* [2004] derived estimates of dense shelf water production from the Adélie Depression. Averaged over the period 1991–2000 the off-shelf flow of dense shelf water in their model is 0.15 Sv when forced with the NCEP-NCAR reanalysis forcing fields. Until now, there have been no direct measurements of the export of dense shelf water from the Adélie Depression. In this paper we report on data from hydrographic moorings that were deployed for almost 2 years (April 1998–February 2000) in the formation and outflow regions. We use these observations to describe the annual cycle of water mass transformations beneath the Mertz Glacier polynya system, presenting time series of salinity and temperature. We use current speed measurements to estimate the volume transport of dense shelf water out of the Adélie Depression. The likely contribution of the dense shelf outflow to the formation of ALBW is discussed.

2. Moored Hydrographic Data

2.1. Mooring Deployment and Instrument Arrays

[8] In April 1998, four moorings were deployed; in July 1999, a second set of moorings was deployed (see

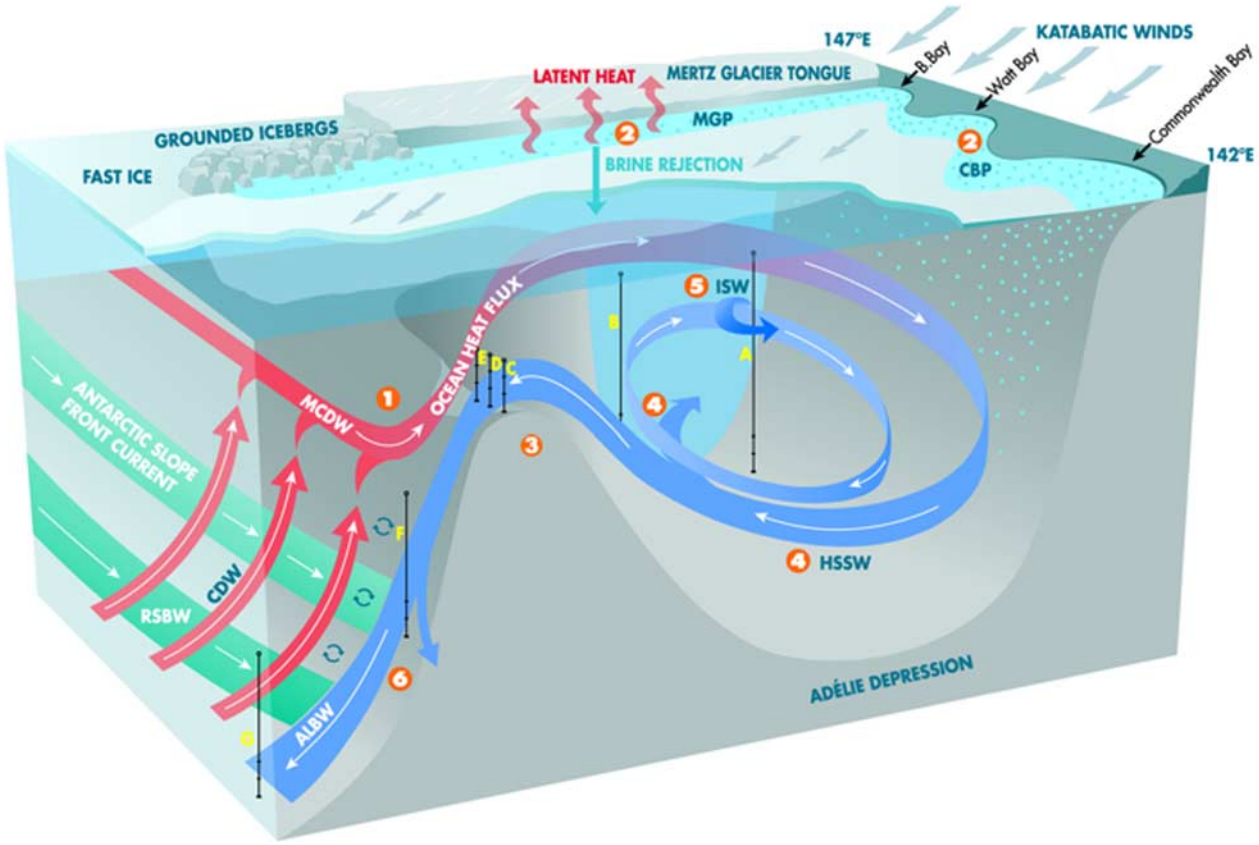

Figure 3. A schematic diagram of the circulation in the Adélie Depression and the processes involved in the production of ALBW [after *Williams*, 2004]. Numbers represent the following: 1, modified Circumpolar Deep Water (MCDW) intrusions; 2, brine rejection beneath Mertz Glacier polynya (MGP) along the Mertz Glacier Tongue (MGT) and in the Coastal Bay polynya (CBP) region including Commonwealth, Watt, and Buchanan bays; 3, dense shelf water export through the Adélie Sill; 4, High-Salinity Shelf Water (HSSW) circulation in the base of depression and beneath the MGT; 5, Ice Shelf Water (ISW) in Buchanan Bay in a cold, fresh westward coastal current; and 6, downslope mixing of dense shelf water in the production of ALBW, eroding the warmer, oxygen-poor, and more saline RSBW from the east. Mooring locations A–E are as shown.

Figures 1b and 4). The moorings were deployed in the center of the Adélie Depression alongside the MGT (see A and B in Figure 4b) and across the Adélie Sill (see C, D, and E in Figure 4a). The moorings span the width of the sill, approximately 20 km south of the minimum sill depth of 420–440 m (see Figure 4a). Mooring D is the deepest site (594 m) in the sill region and includes an upward looking acoustic Doppler current profiler that recorded data from April 1998 to February 2000.

[9] High-quality data were retrieved from 15 temperature-salinity sensors (SBE Microcats) and one upward looking acoustic Doppler current profiler (ADCP) moored in the Adélie Depression from April 1998 to February 2000 (see Table 1). Although the depths between the two recording periods are not identical, two depth classes are well sampled in both years at both the sill and in the depression.

2.2. Temperature-Conductivity Sensors

[10] The principal instruments on the moorings were 15 temperature-conductivity sensors (SBE Microcats), for which the postretrieval processing is detailed by *Rosenberg et al.* [2001]. The sampling time was 5 min in the 1998–1999 deployment, and 7.5 min for the 1999–2000 deployment. The time series of the salinity data show significant spiking [*Rosenberg et al.*, 2001]. In cold waters around Antarctica relatively small errors in temperature or conductivity can strongly affect the salinity calculation resulting in spikes. A damped least squares solution was used to reduce the noise in salinity by estimating a correction temperature to calculate a corrected salinity field [*Williams*, 2004]. This method preferentially minimized the variance associated with the larger salinity spikes, but with consistent temperature changes constrained by the equation for conductivity of seawater. The standard deviation for the RMS variations introduced by this method was ±0.005°C in temperature and ±0.005 in salinity. This corresponds to ±0.004 kg m^{-3} for potential density. The above salinity spiking correction was the only filtering that was applied to the temperature and salinity data from the moorings (after standard quality control and calibration).

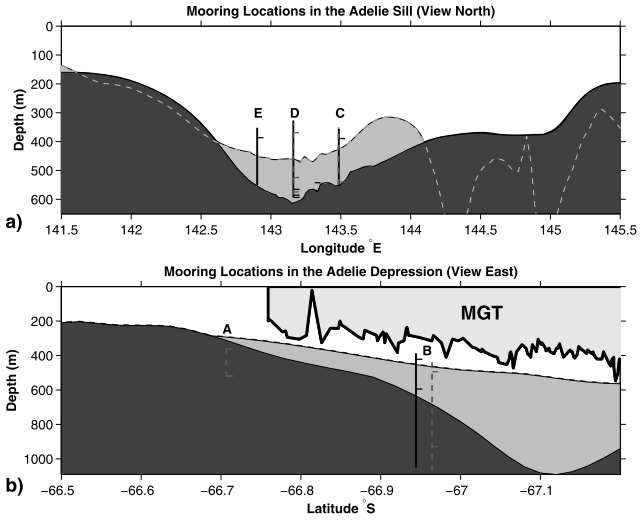

Figure 4. Instrument positions of AU9901 moorings in 1998–1999 (black) and 1999–2000 (grey). (a) Mooring locations (E–C) in the Adélie Sill (view north). The bathymetry shown is for the line of constant latitude running through the mooring locations (dark grey) and the minimum sill depth (light grey). (b) Mooring locations (A and B) in the Adélie Depression against the Mertz Glacier Tongue (MGT). The bathymetry shown is along the line between the moorings (dark grey) and on the eastern side of the MGT (light grey). The MGT is labeled, its thickness taken from *Legrésy et al.* [2004]. The positions of the instruments (detailed in Table 1) are shown by a horizontal dash line.

[11] The moorings were not equipped with pressure sensors and therefore vertical movement of the sensors because of the tilt of the mooring introduced an additional uncertainty. Using the actual mooring design (float buoyancy, instrument location, wire type and mass), modeling the movement of the mooring in a mean current of 20 cm s^{-1} shows a maximum vertical fluctuation in pressure of 5 dbar for the shallowest instrument (note that the fluctuation decreases with depth). For salinity, this depth excursion, would lead to a salinity bias of up to 0.003 and also translates to a bias of 0.001°C in potential temperature. A worst case scenario of a current speed of 1 m s^{-1} results in a vertical displacement >150 m, and an error in salinity of 0.015. These salinity biases are small compared to the seasonal variability that is described here and for these relatively short moorings the effect of mooring motion can be neglected in this paper.

2.3. Acoustic Doppler Current Profile Data

[12] The ADCP deployed in the Adélie Sill (mooring D), was an RD Instruments 150 kHz Broadband (Serial 1143). The ADCP operated in burst mode every 45 min (average over fifteen pings at one ping per second). The major challenge of observing the currents at this location was in measuring the current direction. Accordingly, the ADCP was attached to the anchor in such away to prevent it rotating during the entire deployment period and the instrument heading data was saved in beam coordinates for conversion into Earth coordinates during postprocessing. The average instrument heading over the deployment period was 11.8° ± 2.6° and suggests that the deviation in direction due to the magnetic field fluctuations was relatively small. However the close proximity of the south magnetic pole means that even small tilts (16.9° ± 0.9° over the record) of the instrument cause the ungimballed compass to record apparently large horizontal components of the magnetic field. Consequently, we cannot rely on the orientation of the instrument even though the processed ADCP currents have flow directions that agree with the inferred flow directions from CTD data, model results and aligns with the bathymetry of the region (see discussion below).

[13] We present the apparent mean east/west and north/south velocity components at each bin in Figure 5. There was a seasonal cycle to the mean range of the ADCP instrument that decreased each winter/spring to a minimum of approximately 500 m depth in December 1998 and November 1999, and then increased through the summer/autumn period. This could be related to the amount of biological backscatter in the water column, albeit in a lagged response at depth to the spring phytoplankton bloom. Alternatively it could be due to seasonal variations in vertical shear, as reported in the Denmark Strait Overflow by *Macrander et al.* [2007]. The mean apparent meridional component is northward and peaks above the

Table 1. Details of the AU9901 Mertz Polynya Experiment[a]

Mooring Site	Depth, m	Location	Data Collection Period	Instrument	Depth, m
A	525	66°42′S 145°17′E	31/07/99 to 13/02/00	m-908	355
			31/07/99 to 13/02/00	m-909	510
B	1050	66°57′S 144°56′E	18/04/98 to 1/05/99	m-327	414
			17/04/98 to 11/05/99	m-329	587
B	1071	66°58′S 144°58′E	31/07/99 to 13/02/00	m-1120	486
			31/07/99 to 13/02/00	m-1121	921
C	555	66°12′S 143°29′E	17/04/98 to 14/05/99	m-325	385
			17/04/98 to 8/05/99	m-326	538
C	555	66°12′S 143°29′E	28/07/99 to 13/02/00	m-1119	535
D	594	66°12′S 143°10′E	17/04/98 to 30/04/99	m-323	561
			17/04/98 to 11/05/99	m-324	576
			18/04/98 to 19/02/00	ADCP-1143	589
D	585	66°12′S 143°10′E	28/07/99 to 13/02/00	m-911	365
			28/07/99 to 13/02/00	m-912	520
			28/07/99 to 313/02/00	m-913	570
E	552	66°12′S 142°54′E	17/04/98 to 11/05/99	m-319	386

[a]See Figure 4. At sites B, C, and D, there were moorings in both 1998–1999 and 1999–2000. For further information see *Rosenberg et al.* [2001].

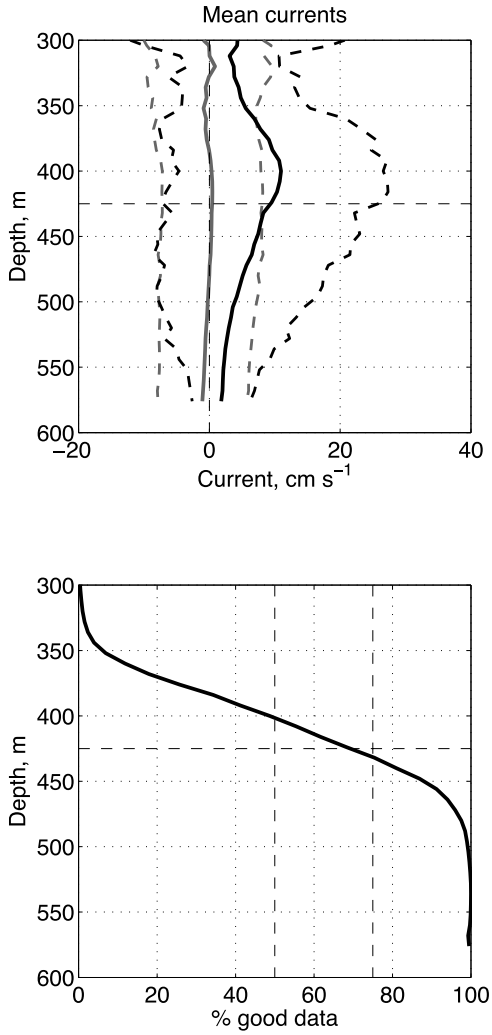

Figure 5. Vertical distribution of mean ADCP currents. (top) Apparent mean u cm s^{-1} (east/west, grey line) and apparent v cm s^{-1} (north/south, solid line) currents at each bin over the entire record, with dashed lines indicating the first standard deviation. (bottom) Percentage of good data points at each bin. The dashed vertical lines indicate 50% and 75%. The horizontal dashed line is the estimated depth of the Adélie Sill.

sill depth at 10cm s^{-1}. The mean zonal component is near zero. This outflow agrees with the ship-based observations [*Williams and Bindoff*, 2003] and numerical modeling [*Marsland et al.*, 2004]. The flow direction also aligns with the bathymetry. Because we cannot be certain of the direction we present currents from the ADCP instrument (without tide signals removed) as speed only and assume that the mean flow past the ADCP instrument is off the shelf.

3. Formation of Dense Shelf Water

[14] Temperature and salinity records from April 1998 to February 2000 are shown in Figures 6 and 7. The results are grouped into shallow (355–486 m, Figure 6) and deep (510–921 m, Figure 7) instrument ranges. The moorings (labeled A–E) are described in a clockwise sequence following the general circulation of inflow across the shelf break (A), into the Adélie Depression (B) and out through the Adélie Sill (C–E). This is the pathway that has been inferred from hydrographic observations of the depression during winter [*Williams and Bindoff*, 2003] and from numerical modeling studies of the region [*Marsland et al.*, 2004]. Owing to the limited temporal coverage of the 1999–2000 instruments we will concentrate on the annual cycle recorded by the 1998–1999 moorings unless otherwise specified.

[15] Salinity increases at each instrument from May to October in response to brine rejection from sea ice growth and decreases between November and April (Figures 6 and 7). This process is relatively symmetric around October for the instruments in the sill region (C, D and E). In contrast, salinity at the shallow instrument at mooring B in the depression decreases sharply in early December. The overall pattern is coherent between the shallow and deep instruments, though the signal is greater in the shallow depth range. The deepest instrument at mooring B (921 m) is adjacent to the MGT and shows high-salinity values for the six month period between August and February.

[16] Temperature at all instruments is close to the surface freezing point (−1.91°C) during the winter sea ice growth period from May through October. Warmer temperatures (0.5–1.5°C above freezing) are observed from December through to March and are indicative of inflowing MCDW. The warmest temperatures are observed near the MGT (moorings A and B), consistent with the enhanced inflow of MCDW on the eastern side of the depression [*Williams and Bindoff*, 2003]. A striking feature of the records from deeper instruments (Figure 7), is the absence of the MCDW in summer. Temperatures in the sill (C and D, Figure 7) warm by only 0.1°C in January–March 1999. Against the MGT (B, Figure 7), the water at 587 m is below the surface freezing point by 0.1–0.2°C between December 1998 and March 1999, indicative of the cooling influence of Ice Shelf Water (ISW). Temperature at the deepest instrument is nearly constant at the surface freezing point throughout the year and does not show any effect of ISW.

[17] In considering the variability of shelf water density available for export, a conceptual model for the seasonal oceanography of the Adélie Depression is constructed with four stages; formation (April–September), peak (October–November), destruction (December) and conditioning (January–March). Owing to the irregular vertical positioning of the instruments on the various moorings, the temperature and salinity were linearly interpolated to two common depth levels, namely, 425 m and 575 m. Figure 8 shows the time series of potential density at these two depths (for 1998 and 1999), for the average of moorings (A and B) in the depression, and the average of the moorings (C–E) in the Adélie Sill.

3.1. April–September: Sea Ice Growth and Brine Rejection

[18] From the end of the austral autumn in April–May, enhanced brine rejection from sea ice growth in the polynyas increases the salinity and density at all instru-

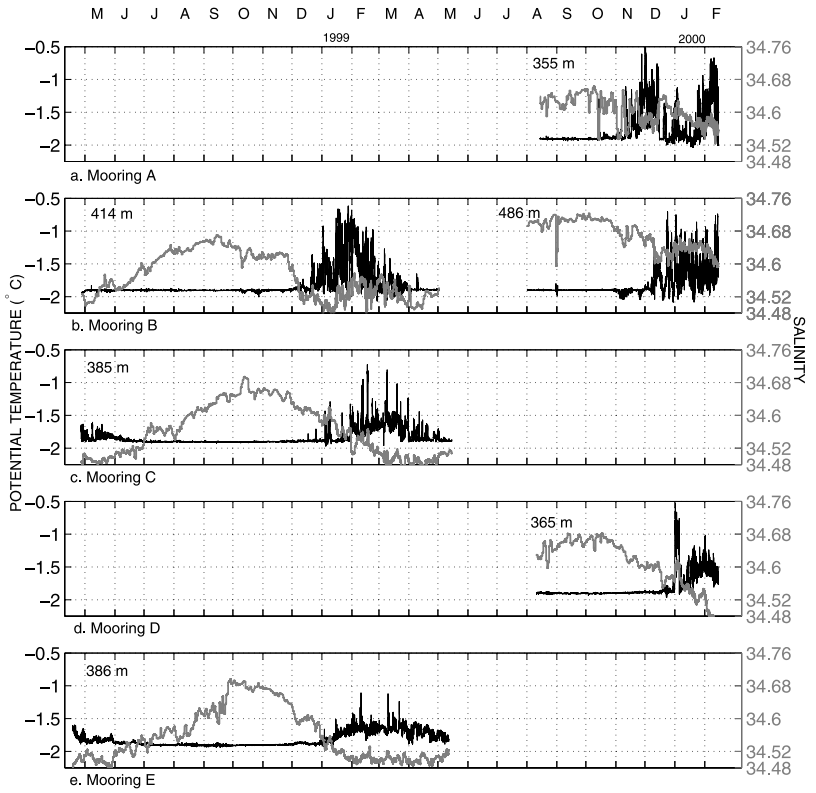

Figure 6. Time series of temperature (solid lines) and salinity (grey lines) for all shallow microcats (Table 1) at mooring locations shown in Figures 1b and 4. (a–e) Mooring locations A–E. Instrument depths are as shown. Dates are from May 1998 to February 2000.

ments. We call this the formation phase. The brine rejection drives convection and erodes the temperature signal of both MCDW intrusions and ISW production (Figures 6 and 7). In the depression beneath the Mertz polynya, the vertical gradient in potential density between the depth levels is a minimum during this period (grey lines in Figure 8), the result of strong vertical mixing. Potential density increases from 27.79 to 27.92 kg m^{-3} between May and September.

[19] At the sill, the water column is not well mixed. In particular, there is greater stratification between the 425 and

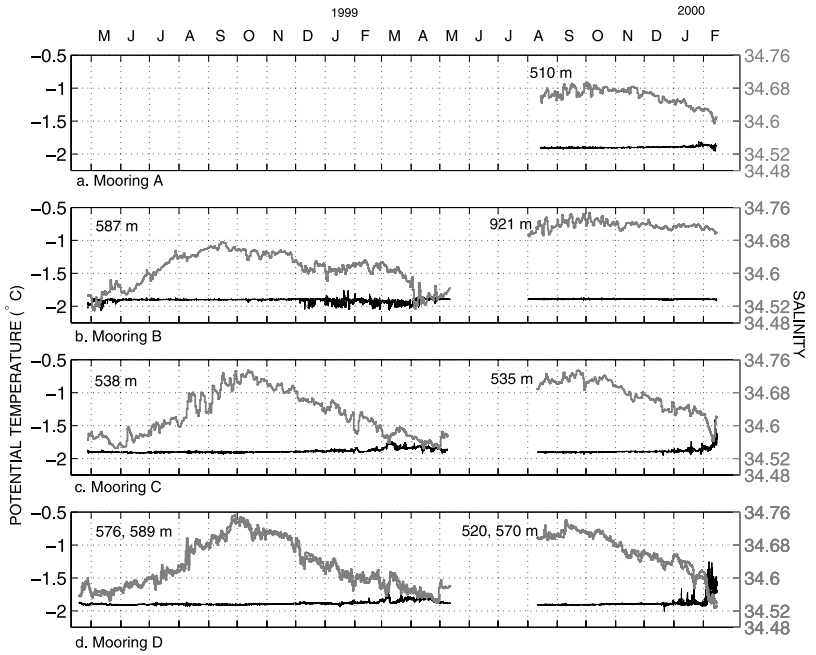

Figure 7. As in Figure 6 but for the deeper instruments.

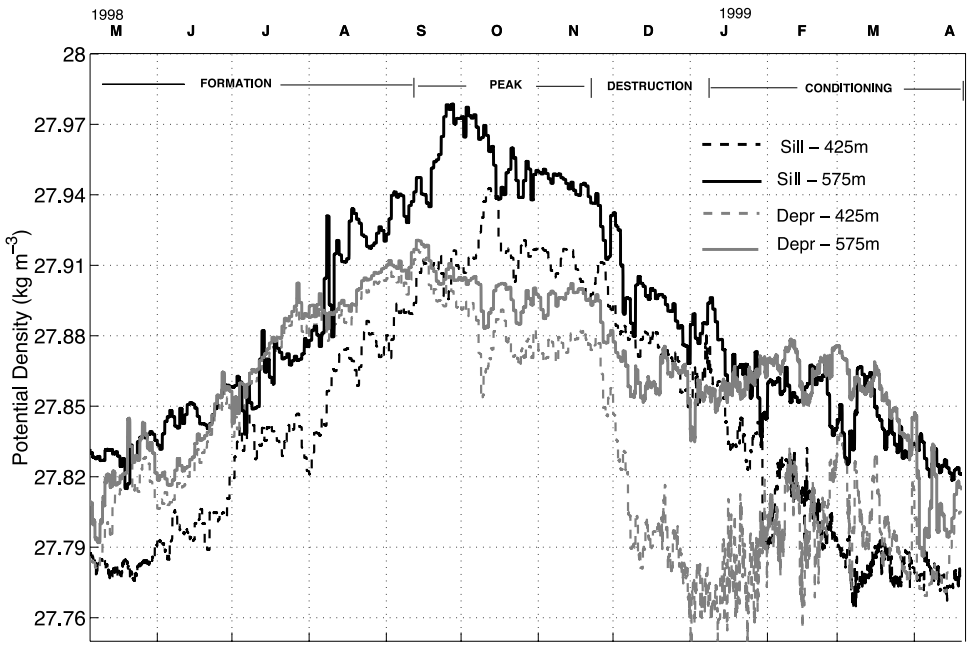

Figure 8. Time series of potential density (σ_θ, kg m^{-3}). These data represent the linear interpolation of all mooring temperature and salinity data (Figures 6 and 7) onto two specific depth levels, 425 and 575 m, for two locations: across the Adélie Depression (moorings A and B, grey dashed line, 425 m, and grey line, 575 m) and across the Adélie Sill (moorings C–E, solid dashed line, 425 m, and solid line, 575 m).

575 m depth levels. The density at 425 m is consistently 0.03 kg m^{-3} lighter than at 575 m. The density at 575 m in the sill is close to that in the depression until August when the density at the sill continues to rise while the density in the depression starts to level out. The maximum density at the sill (575 m) occurs at the end of September when density is more than 0.06 kg m^{-3} greater than in the depression. The peak at 425 m occurs 2 weeks after the peak at 575 m. The timing and magnitude of density increases at the sill reflect the distance of the sill from the formation region at the MGT polynya, and the additional formation of dense water in polynyas along the coastal bays to the west of the MGT, including Commonwealth Bay.

3.2. October–November: Decreasing Brine Rejection and Increasing Ice Shelf Water Influence

[20] The peak period for shelf water densities is in October–November (Figure 8). From ship-based and satellite observations, there is a peak period in the seasonal sea ice cover where the system moves from growth, to stasis, and then melt. Sea ice is still forming from October to November and yet salinity in the depression stops increasing. The plateau in density indicates that salinity enhancement by brine rejection is compensated by export of saline water or input of low-salinity water from either MCDW or ISW. ISW first appears in early October at mooring B, as indicated by small departures of temperature below the surface freezing line in Figures 6 and 7.

[21] At mooring B the cooling and freshening impact of the ISW results in a net decrease in density. Salinity at the shallower depth (Figure 6, 414 m) decreases significantly more than at the deeper instrument (Figure 7, 587 m) in a series of sharp steps that coincide with the appearance of temperatures below the near surface freezing point in October.

3.3. November–December: End of Convection and Beginning of MCDW Advection

[22] After the peak in salinity from October through November, the distribution of water masses changes abruptly (Figures 6 and 7). In the last week of November through December 1998 there is a significant decrease in density of the waters in the depression (see grey lines in Figure 8). This new stratification allows the intrusion of the MCDW southward into the depression to begin from December in 1998, and from November in 1999 as indicated by water as warm as −1°C reaching the shallow instruments on moorings A and B (Figure 6).

[23] Restratification of the water column results in the increased influence of MCDW intrusions in summer. In winter, the intrusions are highly modified and almost all of the warming and freshening signal is removed after the mixing of these intrusions with the dense shelf waters across the shelf break [*Williams and Bindoff*, 2003]. When brine rejection is sufficient to induce convection, the upper water column is well mixed and the warm signature of the MCDW inflow is eroded. After the sea ice regime switches from growth to melt the surface layer becomes lighter and the vertical mixing due to convection stops. This new stratification allows the conspicuous intrusion of MCDW signal southward into the depression from December in 1998 and November in 1999 as indicated by water as warm as −1°C reaching the shallow instruments on moorings A and B (Figure 6).

[24] There is also a seasonal change in the properties of MCDW flowing across the shelf break. In winter, the MCDW is fresher and only slightly warmer than the local

shelf waters as it enters the Adélie Depression on the eastern side of the Adélie Sill after being transported west along the shelf break [*Williams and Bindoff*, 2003]. This westward transport is influenced by the line of grounded icebergs that extend from the front of the MGT (see Figure 2) which become joined by fast ice each winter. This fast ice between the grounded icebergs breaks up in late spring [*Massom et al.*, 2001]. The removal of this fast ice barrier and surface restratification results in the MCDW moving into the depression further to the east of the sill. Any shortening of its mixing pathway into the depression will reduce the decrease in temperature from mixing with the remnant winter shelf waters. The water mass properties of the MCDW intrusions evolve further after December tending to fresher and warmer values in 1999 and fresher values in 2000.

3.4. January–March: Sea Ice Melt, Atmospheric Cooling, and Surface Layer Overturning

[25] A number of processes interact in late summer/early autumn to modify the water column for the following year's formation period. From observations in January 2001 aboard the R/V *Nathaniel B. Palmer*, the summertime stratification over the shelf is one of a seasonal summer mixed layer of relatively warm, fresh, oxygen-rich water above a cold remnant winter layer (T_{min} layer) and below the T_{min} layer intrusions of MCDW at mid depths [*Vaillancourt et al.*, 2003; *Sambrotto et al.*, 2003]. In March and April, the surface waters cool again and there is a new overturning of the water column that mixes the now cooler, fresher AASW with the warm, relatively saline MCDW below. This reduces the salinity beneath the surface layer and returns the upper part of the water column to near-freezing temperatures. Sea ice forms again and starts the next season's production of dense shelf water through brine rejection and vertical mixing.

[26] An increase in salinity in the depression at 414 m (mooring B) after mid-January (Figure 6) is accompanied by an increase in temperature above freezing (up to $-0.5°C$) from mid-January to the beginning of February. The salinity increases through this summer period and peaks toward the end of February. These warm and more saline waters are MCDW. The salinity at 414 m is eroded again during March, but it is still higher than it was at the end of December 1998. These decreases in salinity coincide with waters colder than the surface freezing point, indicative of ISW, freshening the water column.

[27] In Figure 8, the potential density in the depression at 425 m (grey dashed line) increases from 27.77 to 27.84 kg m^{-3} from January to the end of February 1999. Over the same period, the potential density at 575 m (thick grey line) increases from 27.86 to 27.88 kg m^{-3}. These measurements suggest that during the summertime, the upper shelf waters are now receiving extra salinity from the transport of MCDW across the shelf. This is the opposite effect to winter/spring each year when the MCDW inflow is fresher than the local shelf waters.

[28] During March through April, the density in both regions and at both depths decreases, albeit with minor fluctuations. Finally the shelf waters become lighter near the MGT relative to those at the sill. The decrease in salinity in late March corresponds to the cooling of the water column back to the near surface freezing point. The return of cold, fresh values to the 414 m depth in March (Figure 6) is due to the convection of cold, fresh AASW from the surface to 414 m, resulting from surface cooling and increased katabatic winds (not shown).

3.5. Observed Differences in the Sea Ice Regime Between 1998 and 1999

[29] Despite the limited data collected for the 1999–2000 season, we found that the shelf water was more saline in August 1999 relative to 1998, and that the warming signal of MCDW intrusions occurred earlier in 1999 (November) relative to 1998 (December). We examined an analysis of open water area in the Adélie Depression from SSM/I satellite data using the *Markus and Burns* [1995] algorithm (not shown). The mean open water area was approximately 50% greater in 1998 than in 1999 for the period 1 April to 1 October. However in the formation period between 1 May and 1 August, the open water area for 1998 was only 10% greater than 1999. We were therefore unable to determine whether the observed increase in salinity in the Adélie Sill for August 1999 relative to 1998 was the result of increased sea ice production or if there was conditioning of the water column by the previous sea ice growth season in 1998.

[30] *Massom et al.* [2003] describe an extraordinary "breakout" event with the northeast advection of sea ice away from the Adélie region in October 1999. This is after the growth period and therefore is not a factor in the differences in salinity between the 1998 and 1999. However it could be important to the change in timing of the MCDW instrusions, which was noted by the arrival of warm water up to a month earlier in 1999 (November). *Massom et al.* [2003] show the sea ice in the depression was advected northward very quickly after the thicker ice barrier to the north disintegrated. We speculate that this was accompanied by a northward surface transport that enhanced the southward transport of the MCDW.

4. Dense Shelf Water Export

[31] We present time series of current speed (cm s^{-1}) at four depths at and below the Adélie Sill (424, 480, 528 and 576 m) in Figure 9. There is a pattern of vertical homogeneity from the bottom up, overlaid with an additional signal that varies seasonally and has larger amplitude at the shallower depths. The seasonal variability in the range of the ADCP (see section 2) causes the data gaps at the shallowest depth (424 m) in November–December 1998. Maximum mean currents are generally in the range 20–40 cm s^{-1} between August and January, though the raw data often exceed 50 cm s^{-1} at depths of 424 and 480 m. Examining the record at 480 m, we find that the export speed is a maximum from October through December in 1998 and for a shorter period (October through November) in 1999, but with higher peak values. Tides were not removed from these data, however tidal analysis was completed on the original current components derived by the 2-D compass (not shown) and found to have negligible impact on the absolute speeds.

[32] The density measurements from the temperature-salinity sensors and the ADCP current data are combined to estimate the export rate of dense water from the Adélie

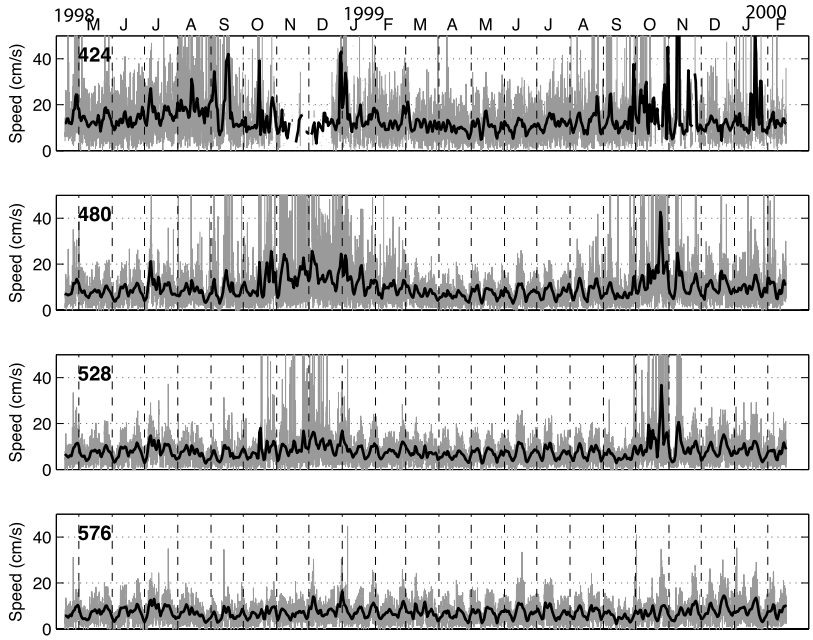

Figure 9. Time series of ADCP speed in cm s^{-1} (grey) with a 2-d running mean (solid line) at (top to bottom) 424 (sill depth), 480, 528, and 576 m. The gaps in the 424 m depth time series occurred when the seasonal variability in the range of the ADCP was inadequate.

Depression. We based our estimate of the export speed on the available data from the range of the ADCP. At times of maximum range, the maximum speed of the water column was above the sill depth. Therefore our estimate, based on the data below the sill depth when the range was a minimum, is likely to be conservative, in particular as this generally occurred during the times of peak shelf water density. The current meter flow speeds are combined with an estimate of the cross-sectional area of the outflow region. In this case the Adélie Sill is assumed to be the only outflow region from the Adélie Depression and that the water exported at the sill depth is correctly identified as the dense water mass that mixes down the continental slope to form the ALBW as observed [*Fukamachi et al.*, 2000].

[33] To assess the potential for ALBW formation, the export rates across the range of observed density classes (27.79 to 27.94 in 0.01 kg m^{-3} increments) are estimated and presented in Table 2. The second set of data from 1999–2000 begins in August and the 27.90 kg m^{-3} density occurs a month earlier than in 1998. There are 16 more days of outflow greater than 27.90 kg m^{-3} in 1999 (101 d) relative to 1998 (85 d). The mean current speed during periods where there is an outflow is between 6.98–12.80 cm s^{-1}. A low number of export days frequently

Table 2. Duration, Timing, and Current Speeds of Exported Shelf Waters in σ_θ Classes[a]

	Number of Days at σ_θ Class		Initial/Final Date of σ_θ Class at Sill		Mean Speed, cm s^{-1}	
σ_θ Class, kg m^{-3}	1998–1999	1999–2000	April 1998 to April 1999	August 1999 to February 2000	April 1998 to April 1999	April 1999 to April 2000
27.79	59	-	21 Apr to 10 Apr	-	6.98	-
27.80	33	-	29 Apr to 21 Mar	-	7.69	-
27.81	18	-	8 Jun to 27 Feb	-	8.13	-
27.82	10	-	30 Jun to 18 Feb	-	9.34	-
27.83	16	-	2 Jul to 12 Feb	-	8.75	-
27.84	33	-	3 Jul to 27 Jan	-	10.22	-
27.85	12	-	8 Jul to 29 Jan	-	11.56	-
27.86	13	-	9 Aug to 14 Jan	-	12.80	-
27.87	18	-	10 Aug to 10 Jan	-	9.68	-
27.88	31	-	13 Aug to 8 Jan	-	11.10	-
27.89	11	-	24 Aug to 18 Dec	-	9.80	-
27.90	17	16	5 Sep to 1 Dec	2 Aug to 10 Nov	9.32	11.72
27.91	29	19	14 Sep to 28 Nov	8 Aug to 6 Nov	9.59	10.74
27.92	32	26	15 Sep to 15 Nov	17 Aug to 28 Oct	8.62	9.04
27.93	2	31	9 Oct to 16 Oct	18 Aug to 21 Oct	8.11	7.58
27.94	5	9	10 Oct to 15 Oct	10 Sep to 17 Oct	8.36	8.78

[a]Two periods are assessed for the buildup and decrease of shelf water σ_θ: between April 1998 and April 1999 and between August 1999 and February 2000. Shown for each 0.01 kg m^{-3} σ_θ class (27.79–27.94 in 1998–1999) are the total number of days during which that σ_θ class is being exported at the sill depth; the date each σ_θ class first reaches the sill depth; the final date at which the σ_θ class is recorded at the sill depth; and the mean speed of the export current (cm s^{-1}) over the export days for each σ_θ class. The 1999–2000 σ_θ classes are limited to 27.90–27.94 because of the late start date in August 1999.

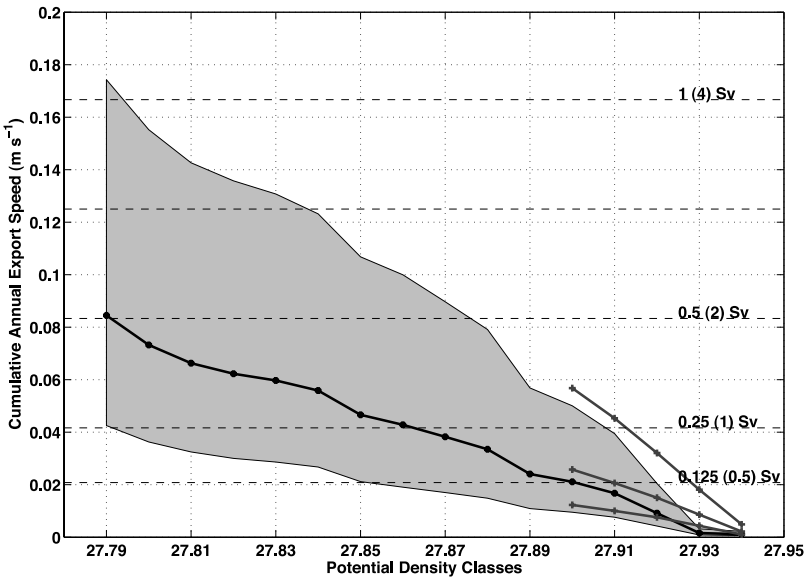

Figure 10. Cumulative annual export speed in density classes. The thick black line with circles represents the estimated mean daily export current in 1998 and is calculated over the available vertical range at and below the Adélie Sill depth for each density class (0.01 kg m^{-3}) in the range 27.79–27.94 kg m^{-3}. The grey area is the expected range using the maximum and minimum vertical daily mean export speed measured. Dashed horizontal lines represent the estimated outflow and downslope production after entrainment (fourfold volume increase in brackets) for an outflow area 40 km by 150 m. A limited set of results is shown for 1999 (dark grey lines with plus signs indicate minimum, mean, and maximum values).

represents periods of increased dense shelf water formation (the shelf waters move rapidly through several density classes). These periods can be understood as the enhanced air-sea interaction and sea ice growth and subsequent convection from brine rejection increasing the density of the shelf waters, and in turn increasing the gyre circulation within the depression.

[34] The cumulative annual export speeds for Table 2 are shown in Figure 10. The outflow area is conservatively estimated as having an area of 6×10^6 m^2. The cumulative annual export across all density classes with a density greater or equal to 27.79 kg m^{-3} is 0.25–1 Sv. The cumulative annual export greater than σ_θ = 27.88 kg m^{-3} is 0.1–0.5 Sv. This latter density is the minimum density class for ALBW production suggested by *Bindoff et al.* [2000b]. The limit was based on a direct mixing line in T-S space between shelf and bottom waters from the Adélie Land region. *Williams* [2004] suggests this is an upper limit, and showed that downslope mixing was not linear in T-S space because of the entrainment of slope waters and that a lower limit of 27.85 kg m^{-3} was still capable of producing ALBW. The cumulative annual export of shelf water denser than this lower limit is 0.125–0.65 Sv. In lieu of future work assessing the true critical shelf water density for protobottom water, we defer to the more conservative value 27.88 kg m^{-3} reported by *Bindoff et al.* [2000b].

5. Conclusions

[35] These observations of the seasonal cycle of density, temperature and salinity for an Antarctic Bottom Water formation region are unique. Our direct estimates of the export of dense shelf water are the first for the Adélie Depression. The observations show that the annual evolution of shelf water density in the polynya is a complex interaction of the key shelf water masses (modified Circumpolar Deep Water, Ice Shelf Water and Antarctic Surface Water) that all effect the density and its seasonal cycle. The formation period begins in April and is characterized by increasing shelf water density in the depression from sea ice formation and peaks in September. Density is then eroded by cool, fresh Ice Shelf Water and then in turn by warm, relatively fresh modified Circumpolar Deep Water, from November through March. The densest water was observed in the outflow region of the Adélie Sill, indicating the influence of additional brine rejection in the Commonwealth Bay polynya. These observations confirm the Adélie Depression as the source of the bottom waters reported by *Fukamachi et al.* [2000] from temperature and speed observations on the continental slope at 2600 m to the west northwest of the Adélie Sill.

[36] Using current speed measurements from a mooring in the outflow region of the Adélie Sill, we present the export in potential density classes from the Adélie Depression in 1998. We conservatively estimate the shelf water export available for downslope transport and bottom water production (density classes 27.88 kg m^{-3} and above) to be 0.1–0.5 Sv. Our assumption of northward transport through this region is only feasible because of the shape of the Adélie Depression and its known circulation. For an expected fourfold increase in volume (1:3 mixing ratio) of exported shelf waters during mixing down the continental slope, we estimate that the Adélie Depression produces 0.4–2.0 Sv of Adélie Land Bottom Water. This indirect estimate of the bottom water formation is broadly consistent with earlier estimates of bottom water production in the Australian-

Antarctic Basin [*Rintoul*, 1998]. *Marsland et al.* [2004] found that in the 10 year period 1991–2001, 1998–1999 were relatively weak years for production of HSSW, and so this export rate estimated from the observations could be conservative relative to a longer-term mean.

[37] The cooling and freshening reported in this layer by *Whitworth* [2002], *Jacobs et al.* [2002], *Aoki et al.* [2005] and *Rintoul* [2007] does agree with a relative increase in the signal from the Adélie Land Bottom Water source. The reported freshening of Ross Sea Bottom Water by *Jacobs et al.* [2002] also influences the Adélie Land Bottom Water properties and further work is needed to quantify these contributions to the East Antarctic sector from the Ross Sea. Relative to Weddell Sea Bottom Water, the Adélie Land Bottom Water is strongly seasonal in its formation rate, with peak production rates occurring in September–October. This seasonality makes mooring arrays vital to monitoring the strength of Adélie Land Bottom Water formation.

[38] Modeling studies show that the shelf water export from the Adélie Depression has both strong interannual variability [*Marsland et al.*, 2004] and will weaken in response to expected future climate change [*Marsland et al.*, 2007]. Further monitoring of all dense overflows into the basins adjacent to Antarctic is very important for understanding future changes to this component of the southern limb of the overturning circulation. Similar programs already exist in the Arctic, measuring the overflows from the Nordic seas. Indeed, because of its geometry and the significant contribution it makes to the Australian-Antarctic Basin, the Adélie Depression is particularly suited to such a monitoring program.

[39] **Acknowledgments.** This work was supported by the Australian government's Cooperative Research Centres Programme through the late Antarctic Cooperative Research Centre. Logistical support was provided by the Australian National Antarctic Research Expeditions, ASAC grant 2223. The authors would like to thank the officers and crew of the R/V *Aurora Australis* for their professional support in the collection of these observational data; Mark Rosenberg from the Antarctic Cooperative Research Centre for processing all of the AU9901 data; Eric Firing at the University of Hawaii for much appreciated helpful comments, and Lea Crosswell at CSIRO, for production of Figure 3.

References

Aoki, S., S. R. Rintoul, S. Ushio, S. Watanabe, and N. Bindoff (2005), Freshening of Adélie Land Bottom Water near 140°E, *Geophys. Res. Lett.*, *32*, L23601, doi:10.1029/2005GL024246.

Bindoff, N. L., S. R. Rintoul, and R. Massom (2000a), Bottom water formation and polynyas in Adélie Land, Antarctica, *Pap. Proc. R. Soc. Tasmania*, *133*(3), 51–56.

Bindoff, N. L., M. A. Rosenberg, and M. J. Warner (2000b), On the circulation and water masses over the Antarctic continental slope and rise between 80 and 150°E, *Deep Sea Res., Part II*, *47*, 2299–2326.

Bindoff, N. L., G. D. Williams, and I. Allison (2001), Sea-ice growth and water-mass modification in the Mertz Glacier polynya, East Antarctica, during winter, *Ann. Glaciol.*, *33*, 399–406.

Fukamachi, Y., et al. (2000), Seasonal variability of bottom water properties off Adélie Land, Antarctica, *J. Geophys. Res.*, *105*, 6531–6540.

Gordon, A. L. and P. Tchernia (1972), Waters of the continental margin off Adélie coast, Antarctica, in *Antarctic Oceanology II: The Australian-New Zealand Sector*, *Antarct. Res. Ser.*, vol. 19, edited by D. E. Haynes, pp. 59–69, AGU, Washington D. C.

Jacobs, S. S. (2004), Bottom water production and its links with the thermohaline circulation, *Antarct. Sci.*, *16*(4), 427–437.

Jacobs, S. S. (2006), Observations of change in the Southern Ocean, *Philos. Trans. R. Soc. London, Ser. A*, *364*(1844), 1657–1681, doi:10.1098/rsta.2006.1794.

Jacobs, S. S., C. F. Giulivi, and P. A. Mele (2002), Freshening of the Ross Sea during the late 20th century, *Science*, *297*(5580), 386–389.

Legrésy, B., A. Wendt, I. Tabacco, F. Rémy, and R. Dietrich (2004), Influence of tides and tidal currents on the Mertz Glacier, East Antarctica, *J. Glaciol.*, *50*(170), 427–435.

Macrander, A., R. H. Käse, U. Send, H. Valdirmarsson, and S. Jónsson (2007), Spatial and temporal structure of the Denmark Strait Overflow revealed by acoustic observations, *Ocean Dyn.*, *57*(2), 75–89.

Markus, T., and B. A. Burns (1995), Method to estimate subpixel-scale coastal polynyas with satellite passive microwave data, *J. Geophys. Res.*, *100*, 4473–4487.

Marsland, S. J., N. L. Bindoff, G. D. Williams, and W. F. Budd (2004), Modelling water mass formation in the Mertz Glacier polynya and Adélie Depression, East Antarctica, *J. Geophys. Res.*, *109*, C11003, doi:10.1029/2004JC002441.

Marsland, S. J., J. A. Church, N. L. Bindoff, and G. D. Williams (2007), Antarctic coastal polynya response to climate change, *J. Geophys. Res.*, *112*, C07009, doi:10.1029/2005JC003291.

Massom, R. A., K. L. Hill, V. I. Lytle, A. P. Worby, M. J. Paget, and I. Allison (2001), Effects of regional fast-ice and iceberg distributions on the behaviour of the Mertz Glacier polynya, East Antarctica, *Ann. Glaciol.*, *33*, 391–398.

Massom, R. A., K. Jacka, M. J. Pook, C. Fowler, N. Adams, and N. Bindoff (2003), An anomalous late-season change in the regional sea ice regime in the vicinity of the Mertz Glacier polynya, East Antarctica, *J. Geophys. Res.*, *109*(C7), 3212, doi:10.1029/2002JC001354.

Morales Maqueda, M. A., A. J. Willmott, and N. R. T. Biggs (2004), Polynya dynamics: A review of observations and modeling, *Rev. Geophys.*, *42*, RG1004, doi:10.1029/2002RG000116.

Orsi, A. H., W. M. Smethie Jr., and J. L. Bullister (2002), On the total input of Antarctic waters to the deep ocean: A preliminary estimate from chlorofluorocarbon measurements, *J. Geophys. Res.*, *107*(C8), 3122, doi:10.1029/2001JC000976.

Porter-Smith, R. (2003), Bathymetry of the George Vth Land shelf and slope, *Deep Sea Res., Part II*, *50*, 1337–1341.

Rintoul, S. (1998), On the origin and influence of Adélie Land Bottom Water, in *Ocean, Ice and Atmosphere: Interactions at the Antarctic Continental Margin*, *Antarct. Res. Ser.*, vol. 75, edited by S. S. Jacobs and R. F. Weiss, pp. 151–172, AGU, Washington, D. C.

Rintoul, S. (2007), Rapid freshening of Antarctic Bottom Water formed in the Indian and Pacific oceans, *Geophys. Res. Lett.*, *34*, L06606, doi:10.1029/2006GL028550.

Rodman, M., and A. L. Gordon (1982), Southern Ocean bottom water of the Australian-New Zealand sector, *J. Geophys. Res.*, *87*, 5771–5778.

Rosenberg, M. A., N. L. Bindoff, S. Bray, C. Curran, I. Helmond, J. Miller, D. Lachlan, and J. Richman (2001), Mertz Polynya Experiment, Marine Science Cruises AU9807, AU9801, AU9905, AU9901 and TA0051—Oceanographic field measurements and analysis, *Antarct. CRC Res. Rep. 25, 1–90*, Coop. Res. Cent. for Antarct. and the Southern Ocean, Hobart, Tasmania, Australia.

Sambrotto, R. N., A. Matsuda, R. D. Vaillancourt, C. Langdon, M. Brown, C. Measures, S. S. Jacobs, and H. Wells (2003), Summer plankton production and nutrient consumption patterns in the Mertz Glacier region of East Antarctica, *Deep Sea Res., Part II*, *50*, 1393–1414.

Vaillancourt, R. D., R. N. Sambrotto, S. Green, and A. Matsuda (2003), Phytoplankton biomass and photosynthetic competency in the summertime Mertz Glacier region of East Antarctica, *Deep Sea Res., Part II*, *50*, 1415–1440.

Wendler, G., C. Stearns, G. Weidner, G. Dargaud, and T. Parish (1997), On the extraordinary katabatic winds of Adélie Land, *J. Geophys. Res.*, *102*, 4463–4474.

Whitworth, T., III (2002), Two modes of bottom water in the Australian-Antarctic Basin, *Geophys. Res. Lett.*, *29*(5), 1073, doi:10.1029/2001GL014282.

Williams, G. D. (2004), Adélie Land bottom water production, Ph.D. thesis, 269 pp., Univ. of Tasmania, Hobart, Tasmania, Australia.

Williams, G. D., and N. L. Bindoff (2003), Wintertime oceanography of the Adélie Depression, *Deep Sea Res., Part II*, *50*, 1373–1392.

N. L. Bindoff and G. D. Williams, Antarctic Climate and Ecosystems Cooperative Research Centre, Private Bag 80, Hobart, Tas 7001, Australia. (n.bindoff@utas.edu.au; guy.williams@acecrc.org.au)

S. J. Marsland, CSIRO Marine and Atmospheric Research, Private Bag 1, Aspendale, Vic 3195, Australia. (simon.marsland@csiro.au)

S. R. Rintoul, CSIRO Marine and Atmospheric Research, GPO Box 1538, Hobart, Tas 7001, Australia. (steve.rintoul@csiro.au)